Ignition of Isomers of Pentane : An Experimental and Kinetic Modeling Study

Ribaucour, M., Minetti, R., and Sochet, L.R.
Universite des Sciences et Technologies de Lille, UMR CNRS 8522 France

Curran, H. J., Pitz, W. J., and Westbrook, C. K.
Lawrence Livermore National Laboratory, Livermore, CA, USA

Abstract

Experiments in a rapid compression machine have examined the influences of variations in fuel molecular structure on the autoignition of isomers of pentane. Autoignition of stoichiometric mixtures of the three isomers of pentane were studied at compressed gas initial temperatures between 640K and 900K and at precompression pressures of 300 and 400 torrs. Numerical simulations of the same experiments were carried out using a detailed chemical kinetic reaction mechanism. The results are interpreted in terms of a low temperature oxidation mechanism involving addition of molecular oxygen to alkyl and hydroperoxyalkyl radicals. Results indicate that in most cases, the reactive gases experience a two-stage autoignition. The first stage follows a low temperature alkylperoxy radical isomerization pathway that is effectively quenched when the temperature reaches a level where dissociation reactions of alkylperoxy and hydroperoxyalkylperoxy radicals are more rapid than the reverse addition steps. The second stage is controlled by the onset of dissociation of hydrogen peroxide. At the highest compression temperatures achieved, little or no first stage ignition is observed. Particular attention is given to the influence of heat transfer and the importance of regions of variable temperature within the compressed gas volume. Implications of this work on practical ignition problems are discussed.

Introduction

Hydrocarbon ignition is important in many practical combustion systems, including internal combustion engines, detonations, pulse combustors, and flame initiation. The rapid compression machine (RCM) is used frequently to study kinetics of hydrocarbon autoignition [e.g., 1-8], since reactive gas temperatures are similar to those in automotive engines during Diesel ignition and end gas autoignition in spark-ignition engines.

The RCM provides a rich environment for study of hydrocarbon oxidation, including degenerate chain branching, alkylperoxy radical isomerization and thermal feedback [9]. Hydrocarbon oxidation studies in the RCM have been summarized recently [10,11], and many classes of fuels have been studied. Detailed kinetic modeling is another tool to study autoignition in the RCM [4,12]. The present work is intended to determine experimentally the influence of variations in fuel molecular structure on autoignition and use a kinetic model to understand those variations. This study is unique in that while other studies have addressed effects of variations in pressure and equivalence ratio [12], this work addresses effects of variations in fuel molecular structure for all isomers of a single fuel, pentane, in a RCM. The three isomers of pentane possess many of the structural elements that determine such autoignition characteristics as octane number and variability in cool flame production.

Experimental results

The Lille experimental facility rapidly compresses reactive mixtures of hydrocarbon / oxygen / inert by a piston stroke. The overall compression ratio is 9.28, and compression time in this study is 60 ms. The piston stops at the end of its travel (top dead center = TDC) where the reacting mixture remains at constant volume. Pressure-time data during the compression and constant volume periods are measured by a Kistler transducer and recorded at a sampling rate of 25 kHz. Light emission associated with the cool flame is measured by a photomultiplier fitted with a color blue filter. Full details of the apparatus and experimental procedures have been described [13,14].

Pressure and temperature at TDC must be known as precisely as possible. Pressure at TDC is measured experimentally, but temperature at TDC is not readily accessible by measurement and must be calculated from the pressure according to a suitable model. The assumption of adiabatic compression is unrealistic in the present case because at least two factors can alter the temperatures during compression, including heat losses to the chamber walls and heat release from chemical reactions. Experimental pressures at TDC are usually lower than theoretical pressures calculated with the adiabatic law, suggesting that heat losses during compression are greater than reactive heat release.

Therefore, temperatures at the end of compression are calculated from the pressure at TDC, the initial pressure and temperature, the compression ratio and the perfect gas law. Temperatures computed in this manner represent spatial averages

because, due primarily to heat losses to the combustion chamber walls, different regions in the compressed gas have local temperatures that are different from the averaged temperature. Autoignition delay times computed from this average temperature can therefore produce results either longer or even shorter than the experimentally determined values [12].

The reaction mixture at TDC is not homogeneous but includes pockets of hotter gas that do not experience heat loss, as observed by LIF of formaldehyde in an optical motored engine [15]. The adiabatic core gas model [16] is based on the assumption of an adiabatic core zone, surrounded by a boundary zone that cools by heat transfer. Pressure is assumed homogeneous in the chamber, but not the temperature. The core gas volume shrinks with time and vanishes when the reaction time becomes sufficiently long. Temperature at TDC has been measured in the center of the rapid compression machine using laser Rayleigh scattering [17] and agrees well with theoretical adiabatic core-gas temperatures [18] calculated from the initial temperature, pressure at TDC and temperature-dependent specific heats of the reactants. Temperature measurements by thermocouple show that the core gas occupies about 80% of the chamber [19]. Reduced temperature inhomogeneities have been observed before ignition and can be explained by the negative temperature coefficient of reaction through its feedback action on the heat release.

Delay times for the first (cool flame) and second stage ignition of n-pentane, isopentane, and neopentane were deduced from pressure and light emission traces. Reactive mixtures consisted of fuel / oxygen / diluent in the ratio 1 / 8 / 30.08; when the

diluent is N_2, the mixture is stoichiometric pentane / air. To reach compression temperatures over the range 640-900 K, part or all of the nitrogen was replaced by argon or carbon dioxide. For each fuel, twelve stoichiometric mixtures were studied. At least three identical experiments were conducted on each mixture with initial pressures of 300 and 400 torrs. Experimental ignition delay times are plotted versus TDC core gas temperature in Figures 1-3. The autoignition behavior can be characterized by the following quantities: the lowest temperature at which autoignition takes place (T_l), the extent of the negative temperature coefficient (NTC) zone (T_{min}, T_{max}), the minimum and maximum ignition delay times within that zone (t_{min}, t_{max}), and the extent of the cool flame (CF) zone (T_{CFmin}, T_{CFmax}). These values are reported in Table I.

Isopentane (RON = 92.3) is the least reactive pentane isomer, and its ignition delay times in the NTC zone are the longest (Table I). Ignition was not observed below 690 K, a clear negative temperature coefficient of the reaction rate was seen between 730 K and 820 K and the temperature range of 700 – 755K in which cool flames were observed is narrow.

N-pentane (Fig. 3) is the most reactive isomer. Its low octane number (RON = 61.7) is consistent with a low ignition limit T_l of 650 K and the shortest ignition delay times in the NTC zone. The NTC and the cool flame zone extend over wide ranges of temperature: 755-845 K and 665-845 K respectively at 400 torrs.

The ignition limit for neopentane is about 670 K, intermediate between

n-pentane and isopentane, consistent with its octane number (RON = 85.5). However some peculiarities should be noted. The ignition delay decreases slowly with temperature after about 770 K at both initial pressures (Fig. 2), and a negative temperature dependence is not observed. Experiments at 200 torrs (not presented here) showed a weak NTC behavior between 770 and 850 K. In a high pressure flow reactor study of neopentane oxidation, Wang et al. [20] observed NTC behavior but noted it was much less pronounced than n-pentane under comparable conditions.

Another interesting feature of neopentane autoignition is the persistence of cool flame activity over the entire range of investigated temperatures. Moreover, for compression temperatures above 770K, the cool flame occurs during the compression stroke. The measured pressure at TDC is therefore influenced by heat release from the cool flame and results in core gas temperatures about 20 K greater for these cases for neopentane than the other isomers without cool flame behavior during compression.

MODELING OF IGNITION DELAY TIMES

The chemical kinetic reaction mechanisms used for these simulations are based on a long history of mechanism development. Recent modeling studies of n-pentane [4,12,21], neopentane (2,2-dimethyl propane) [20-22], and iso-pentane (2-methyl butane) [21]. These mechanisms are refined continually, but the three mechanisms used here are at the same level and detail as that reported [20] for neopentane. The three mechanisms were combined into a single, larger mechanism which is too large to include here but is

available from the authors. No mechanism modifications were made to alter the computed results or their level of agreement with experimental data.

The numerical model computed reactant evolution through the compression stroke and the subsequent constant volume period. During compression, there is considerable turbulence and mixing of the reactants in the combustion chamber, so heat losses to combustion chamber walls can be presumed distributed rather uniformly throughout the mixture. Once the piston stops, heat losses were assumed to come from gases near the chamber wall, leaving an adiabatic core that retains heat for a longer period of time. Therefore heat losses were included for the compression stroke and neglected during the constant volume period. This assumption should be reasonably valid except for long autoignition times after the end of compression, when heat transfer from the core will render it no longer adiabatic. To include the effects of heat losses to the chamber walls, a non-reactive experiment was carried out, replacing oxygen with additional nitrogen. A time-dependent, distributed heat transfer coefficient was then determined to be used during the compression stroke so the computed pressure history matched the experimental results, as seen in Figure 4.

In another series of model computations, the pressure measured at TDC and the resulting core gas temperature were used as initial conditions, without simulating the compression stroke and considering the system as adiabatic. The results shown as dashed lines in Figs. 1-3 are not very different from those where simulations of reactions during the compression stroke were included. Therefore the concept of a core gas at TDC is a satisfactory approximation for modeling autoignition within the operating

conditions of the Lille RCM, except in those cases where long ignition delay times affect the core temperature.

RESULTS

Computed results are shown as curves in Figs. 1-3, again showing the time of onset of the first stage ignition and the time of the final ignition. Results computed when the compression period was not modeled are shown as dashed curves.

Overall agreement between computed and experimental results is generally very good for both total ignition delay and the time of the first stage ignition. Only for the lower pressure experiments with iso-pentane are differences quantitatively significant, with computations indicating ignition at about 60 ms while experiments showed ignition at about 100 ms. At these long experimental ignition delay times, the assumption in the model of adiabatic conditions may be inaccurate. To test this hypothesis, computed constant-volume portions of these histories were repeated, introducing heat loss with the same rate as used during the compression stroke. With the same heat loss rate, these simulations failed to ignite. Even with smaller rates of heat transfer, these mixtures either failed to ignite, or ignited at very long elapsed times. It is apparent that differences between computed and experimental ignition delay times for iso-pentane are due to uncertainties in the heat transfer treatment in the model and that the adiabatic core in the experimental problem is affected by heat transfer for reaction times of more than about 40 ms. In all cases for the other isomers, ignition was

rapid and vigorous in both the model and experiment, and the adiabatic core was insensitive to heat losses.

The relative behavior of the isomers of pentane is illustrated in Figure 5, showing computed temperatures for each isomer at a compression temperature of 757K and initial pressure of 400 torrs. The compression histories of the three cases are virtually identical, but the constant volume ignitions are quite different. All three show a distinct first stage ignition, but the time delays for that first ignition are very short (2.4 ms) for n-pentane, longer for neopentane (6 ms) and much longer for iso-pentane (7.5 ms). Temperature increase (ΔT = 163K, 106K, 70K, respectively) and fuel consumption (Δfuel = 41%, 21%, 20% respectively) during first stage ignition for n-pentane, neopentane, and iso-pentane are quite different, as is the duration of the first stage ignition (0.7 ms, 3 ms, 2.6 ms, respectively). Onset of the second stage occurs in the same order as expected from octane ratings for these fuels.

For each pentane isomer, low temperature oxidation takes place via alkylperoxy radical isomerization [e.g., 23,24]. At these temperatures, the main reactions for pentane isomers are H atom abstraction from the fuel, primarily by OH

$$C_5H_{12} + OH = C_5H_{11} + H_2O \quad (1)$$

H atom abstraction by OH varies weakly with the type of C – H bond being broken, with primary C – H bonds being somewhat stronger than secondary C – H bonds and tertiary bonds being weakest, so H atom abstraction will produce each type of alkyl

radical possible for each isomer. Processes leading to first stage ignition begin by addition of molecular oxygen to the pentyl radicals:

$$C_5H_{11} + O_2 = C_5H_{11}O_2 \quad (2)$$

Pentylperoxy radicals then isomerize via internal abstraction of H atoms. Rates of these isomerizations depend primarily on two major elements, the type of C-H bond being broken and the number of atoms in the transition state ring through which the H atom is abstracted. The activation energy E_{iso} for isomerization can be written [24] as the sum of ring strain energy E_{rs}, the bond energy for the bond broken E_{bond}, and the endothermicity ΔE of the overall reaction.

$$E_{iso} = E_{rs} + E_{bond} + \Delta E \quad (3)$$

The most reactive pentane isomer is n-pentane,

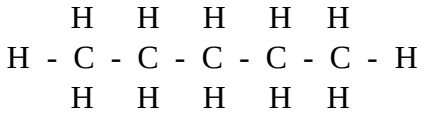

(4)

This molecule can be rewritten to indicate different, logically distinct H atoms:

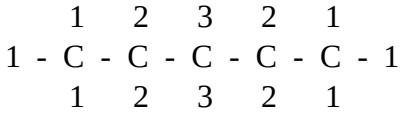

(5)

Isomerization of pentylperoxy radicals in this fuel is facilitated by the ready availability of secondary site H atoms at sites (sites 2 and 3 in the model above) that involve 6-membered transition state rings, because E_{rs} is a minimum for a 6-membered transition

state ring, while E_{bond} is smaller for breaking a secondary bond than a primary bond.

Model computations show that the major products of 1-pentylperoxy and 2-pentylperoxy radical isomerizations are :

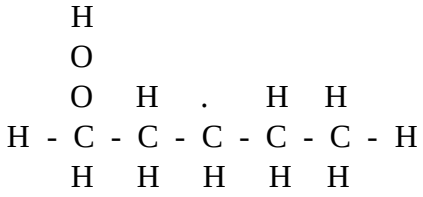

(6)

and

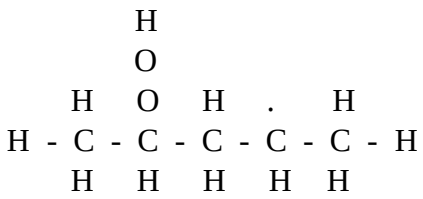

(7)

both favored because they involve 6-membered transition state rings and weakly bound secondary site H atoms (i.e., (1,5s) reactions). The rate of the comparable isomerization of 3-pentylperoxy radicals is relatively inhibited because, although a 6-membered transition state ring structure is attainable, it involves internal abstraction of an H atom from a primary (1,5p) process, rather than a secondary site. Subsequent reaction steps leading to chain branching and rapid reaction involve addition of another O_2 molecule to the QOOH radical site, followed by a series of further internal H atom abstractions, following the principles for activation energy barriers noted above. These final species eventually decompose to produce 3 or more radical species, providing chain branching.

Neopentane is unique in that all of its H atoms involve primary C – H bonds :

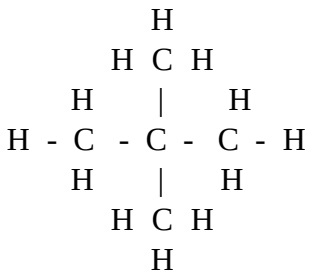

(8)

Following H atom abstraction and addition of molecular oxygen, there are 9 H atoms available for internal abstraction, each of which is relatively strongly bound at primary sites but have the advantage of low activation barrier 6-membered transition state ring locations. That is, the pentylperoxy radical has the structure :

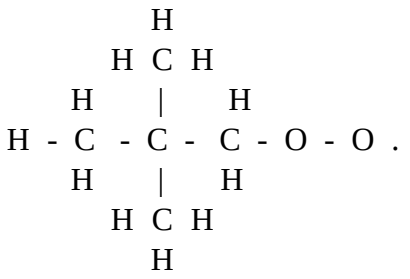

(9)

Although the energy barrier to this (1,5p) H atom abstraction is 1.75 kcal / mole higher than the (1,5s) transfers in n-pentane, there are 9 H atoms available, which facilitates this reaction step and allows the reaction sequence to proceed relatively rapidly. The absence of an NTC regime for neopentane is due in large measure to the fact that there is no conjugate alkene that can be formed by neopentane, due to its highly symmetric and completely primary C – H structure.

Iso-pentane has the structure:

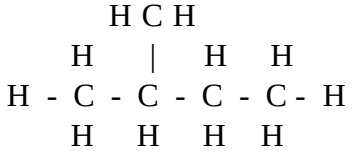

(10)

The most easily abstracted H atom is at the tertiary site. However, subsequent internal H atom abstraction is inhibited relative to neopentane and n-pentane. In neopentane, there are 9 H atoms at primary sites with 6-membered transition state rings, while in iso-pentane, there are only 3 (1,5p) H atoms available. All other internal H atom abstraction reactions in iso-pentane are more inhibited because they involve 5 membered transition state rings, either (1,4p) or (1,4s) reactions, or the initial H atom abstraction is inhibited because it involved the more strongly bound primary C – H bonds. Therefore, the overall rate of chain branching in iso-pentane is lower than that for neopentane by at least a factor of three, and its ignition rate is considerably slower than that of neopentane.

The first stage ignition ends when the temperature has increased enough to reverse the addition reactions of molecular oxygen to alkyl and hydroperoxyalkyl radicals. The alkylperoxy radicals then decompose via lower activation energy chain propagation pathways to produce olefin+OH and epoxide+HO_2 species, effectively shutting off the chain branching reaction pathways, and reaction remains slow until higher temperatures activate new, alternative reaction pathways.

For all three isomers of pentane, the second stage or hot ignition has exactly the same kinetic source. As seen in Figure 5, all three fuels ignite at approximately the same temperature of about 950K. For the pressures of this study, this is the temperature

at which hydrogen peroxide (H_2O_2) decomposes at a significant rate. Low temperature reactions produce an increasing amount of H_2O_2 that is stable until its decomposition temperature is reached; since this reaction is part of the H_2/O_2 reaction submechanism, it is independent of the specific hydrocarbon fuel being studied. Past kinetic modeling studies have demonstrated that this same decomposition reaction is responsible for the onset of knock in spark-ignition engines [21,25,28], ignition in Diesel engines [26,28], and ignition under Homogeneous Charge Compression Ignition (HCCI) conditions [27,28].

Kinetic modeling shows that the isomers of pentane ignite at different times primarily because their different first stage ignitions cause them to arrive at the hot ignition temperature at different times. The most reactive isomer, n-pentane, has the most vigorous first stage ignition and the greatest associated amount of temperature increase, while neo-pentane has a slower first stage ignition with less temperature increase. Iso-pentane has the slowest first stage ignition and the least heat release. These differences in first stage ignition properties are attributable to differences in their molecular structure and the types of C – H bonds in these molecules. Following the end of the first stage ignition, n-pentane is closest to the onset of hot ignition determined by H_2O_2 decomposition.

It is clear that low temperature, alkylperoxy radical isomerization plays a major role in many practical, applied ignition situations, including engine knock and Diesel

ignition. In addition, the overall success of the kinetic model to describe the experimental results indicates that the most important kinetic features of these problems are captured by these reaction mechanisms, in particular the influences of fuel molecular size and structure. Finally, the value of the rapid compression machine to examine these issues has again been confirmed; in addition, this work has been able to examine the sensitivity of some RCM experiments to details in the heat transfer model and spatial inhomogeneities in temperature in the combustion chamber.

REFERENCES

1. Griffiths, J.F., Halford-Maw, P.A., and Rose, D.J., **Combust. Flame** 95, 291-306 (1993).
2. Minetti, R., Ribaucour, M., Carlier, M., Fittschen, C., and Sochet, L.R., **Combust. Flame** 96, 201-211 (1994).
3. Park, P., and Keck, J.C., SAE Paper 900027, 1990.
4. Cox, A., Griffiths, J.F., Mohamed, C., Curran, H.J., Pitz, W.J., and Westbrook, C.K., **Proc. Combust. Inst**. 26 : 2685-2692 (1996)
5. Kirsch, L.J., and Quinn, C.P., **Proc. Combust. Inst.** 16: 233 (1976).
6. Carlier, M., Corre, C., Minetti, R., Pauwels, J.-F., Ribaucour, M., and Sochet, L.-R., **Proc. Combust. Inst.** 23: 1753-1758 (1991).
7. Minetti, R., Carlier, M., Ribaucour, M., Therssen, E., and Sochet, L.-R., **Proc. Combust. Inst.** 26: 747-753 (1996).
8. Minetti, R., Roubaud, A., Therssen, E., Ribaucour, M., and Sochet, L.-R., **Combust. Flame** 118, 213-220 (1999).
9. Griffiths, J.F., and Scott, S.K., **Prog. Energy Combust. Sci.** 13, 161 (1987).
10. Griffiths, J.F., and Mohamed, C., Chapter 6 in Comprehensive Chemical Kinetics (G. Hancock, Ed.), Elsevier, Amsterdam (1999).
11. Griffiths, J.F., **Prog. Energy Combust. Sci.** 21, 25 (1995).
12. Westbrook, C. K., Curran, H. J., Pitz, W. J., Griffiths, J. F., Mohamed, C., and Wo, S. K., **Proc. Combust. Inst.** 27: 371-378 (1998).

13. Ribaucour, M., Minetti, R., and Sochet, L.R., **J. Chim. Phys.** 89:2127-2152 (1992)

14. Minetti, R., Ribaucour, M., and Sochet, L.R., **Combust. Sci. Technol.** 113-114:179-192 (1996)

15. Buerle, B., Hoffmann, F., Behrendt, F., and Warnatz, J., **Proc. Combust. Inst.** 25: 135-141 (1994).

16. Hu, H., Keck, J., SAE paper 87-2110, 1987

17. Desgroux, P., Gasnot, L., and Sochet, L.R., **Appl. Phys.** B61:69-72 (1995)

18. Minetti, R., Ribaucour, M., Carlier, M., Fittschen, C. and and Sochet, L.R., **Comb. Flame.** 96, 201-211 (1994)

19. Desgroux, P., Minetti, R., and Sochet, L.R., **Combust. Sci. Technol.** 113-114:192-303 (1996)

20. Wang, S., Miller, D. L., Cernansky, N. P., Curran, H. J., Pitz, W. J., and Westbrook, C. K., **Comb. Flame** 118, 415-430 (1999).

21. Curran, H. J., Gaffuri, P., Pitz, W. J., Westbrook, C. K., and Leppard, W. R., **Proc. Combust. Inst.** 26: 2669-2677 (1996).

22. Curran, H. J., Pitz, W. J., Westbrook, C. K., Hisham, M. W. M., and Walker, R. W., **Proc. Combust. Inst.** 26: 641-649 (1996).

23. Curran, H. J., Gaffuri, P., Pitz, W. J., and Westbrook, C. K., **Combust. Flame** 114, 149-177 (1998).

24. Pollard, R. T., *Comprehensive Chemical Kinetics, Vol. 17* (C. H. Bamford and C. F. H. Tipper, Eds.), Elsevier, New York (1977).

25. Westbrook, C. K., Pitz, W. J., and Leppard, W. R., SAE Paper 912314, Society of Automotive Engineers (1991).

26. Flynn. P. F., Durrett, R. P., Hunter, G. L., zur Loye, A. O., Akinyemi, O. C., Dec, J. E., and Westbrook, C. K., SAE Paper 1999-01-0509, Society of Automotive Engineers (1999)

27. Aceves, S. M., Flowers, D. L., Westbrook, C. K., Smith, J. R., Pitz, W. J., Dibble, R., Christensen, M., and Johansson, B., SAE Paper 2000-03-0327, Society of Automotive Engineers (2000).

28. Westbrook, C. K., **Proc. Combust. Inst.** 28: xxx-xxx (2000).

LEGENDS

Fig. 1 : Delay times of cool flame and total ignition for stoichiometric mixtures of isopentane / oxygen / inert at initial pressures of 400 (*a*) and 300 (*b*) torrs. Open (cool flame) and filled (total ignition) symbols : experiment, T = core gas temperature at TDC. Solid line: simulation including the compression phase; dashed line: simulation without the compression phase, T = core gas temperature at TDC.

Fig. 2 : Delay times of cool flame and total ignition for stoichiometric mixtures of neopentane / oxygen / inert at initial pressures of 400 (2*a*) and 300 (2*b*) torrs. Open (cool flame) and filled (total ignition) symbols : experiment, T = core gas temperature at TDC. Solid line: simulation including the compression phase, dashed line: simulation without the compression phase, T = core gas temperature at TDC.

Fig. 3 : Delay times of cool flame and total ignition for stoichiometric mixtures of n-pentane / oxygen / inert at initial pressures of 400 (3*a*) and 300 (3*b*) torrs. Open (cool flame) and filled (total ignition) symbols: experiment, T = core gas temperature at TDC. Solid line: simulation including the compression phase, dashed line: simulation without the compression phase, T = core gas temperature at TDC.
Dashed line : simulation without the compression phase, T = core gas temperature at TDC.

Fig. 4 : Pressure history of a non reactive mixture
n-pentane / N_2 / Ar = 0.0256 / 0.2048 / 0.7696. Symbols are experimental values, curve is the simulation, initial conditions : p_0 = 400 torrs, T_0 = 355 K

Fig. 5 : Temperature history for pentane isomers at the same compression temperature.

Table 1 : Autoignition criteria for stoichiometric hydrocarbon / "air" mixtures

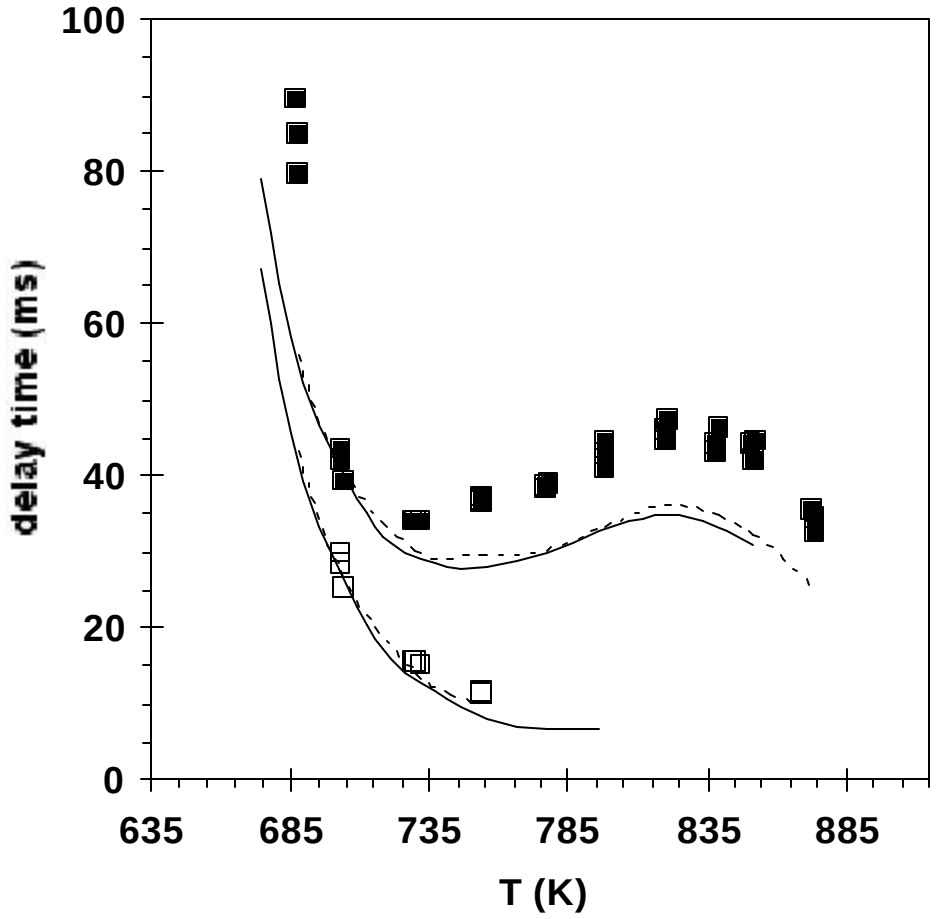

1a

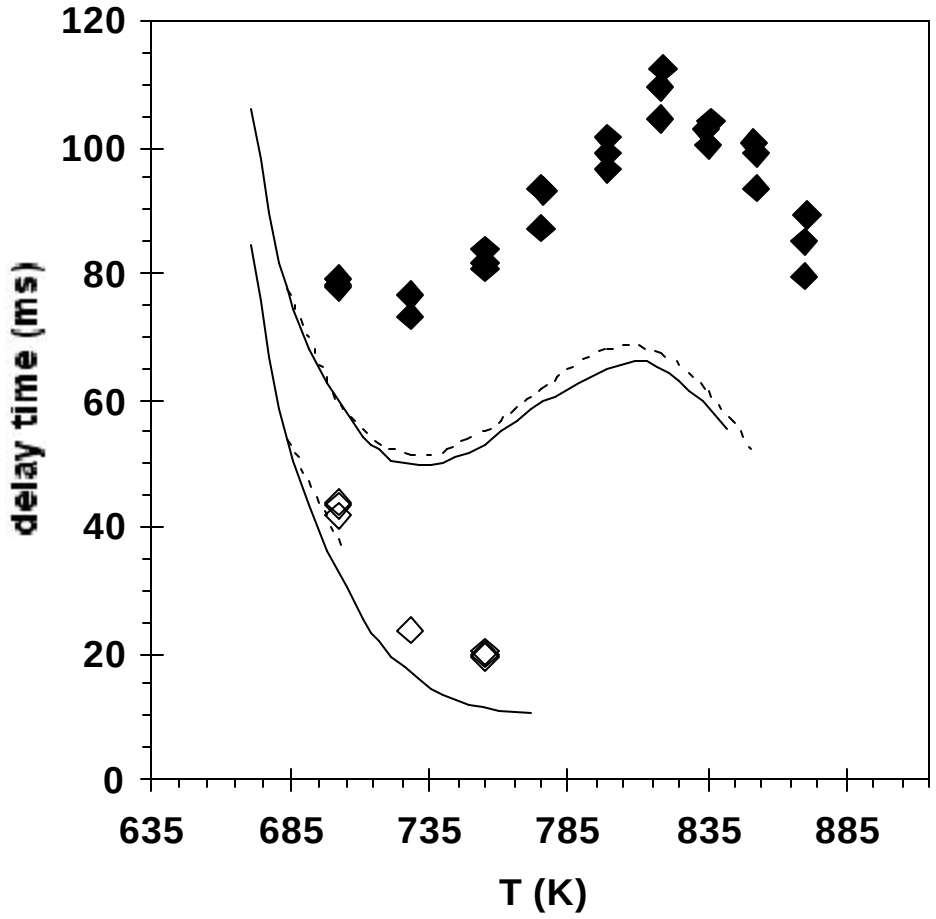

1b

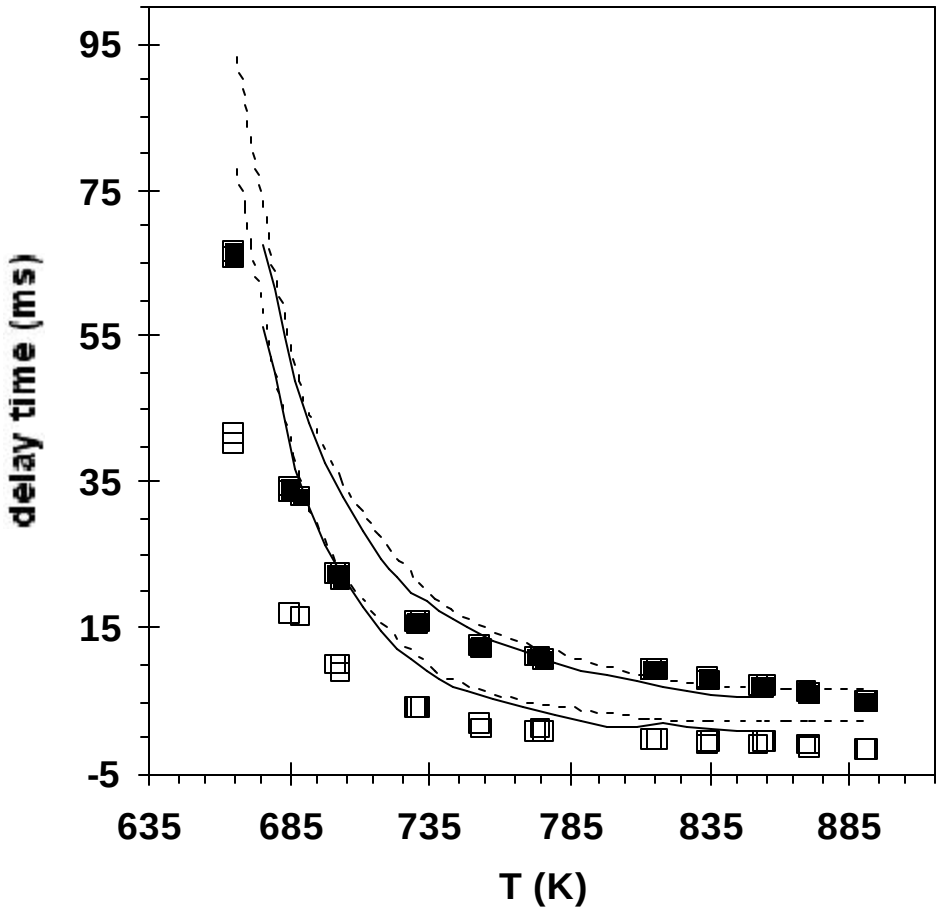

2a

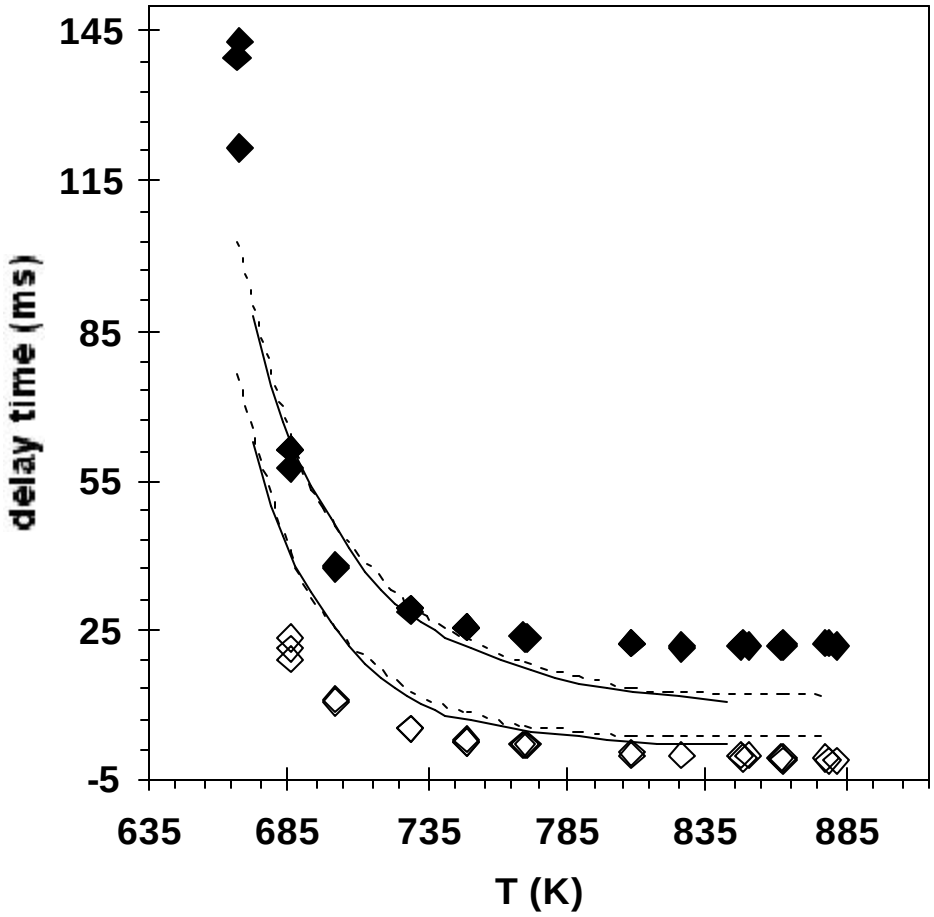

2b

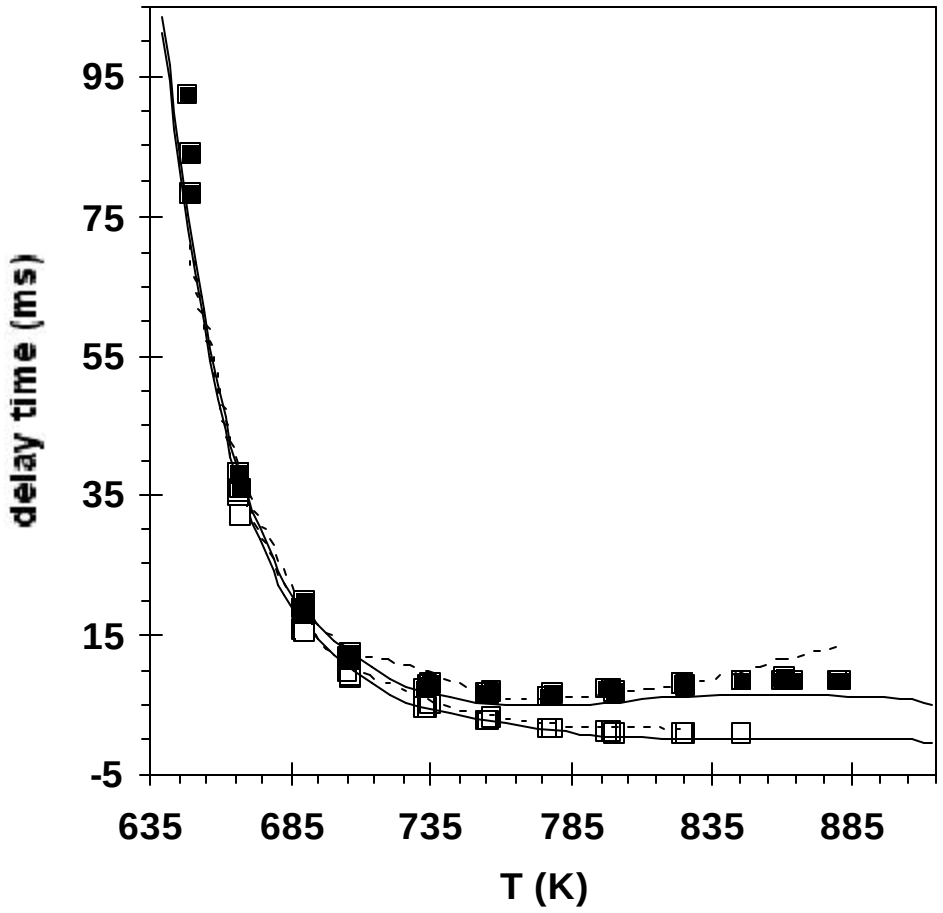

3a

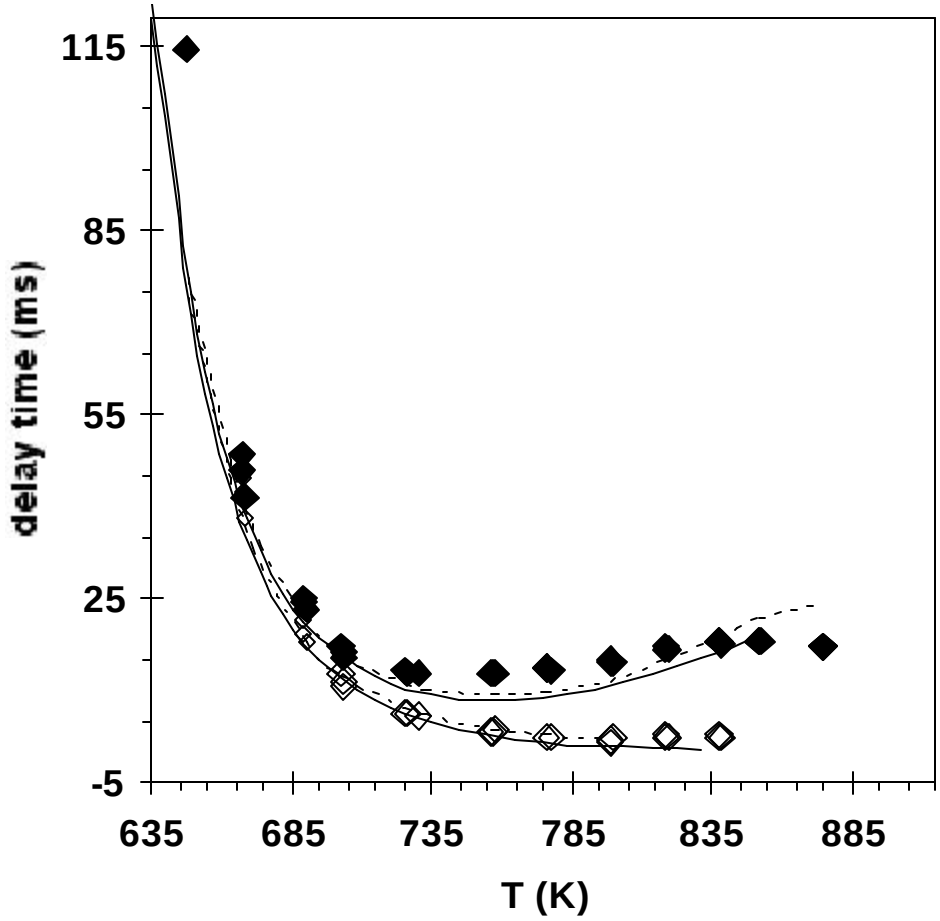

3b

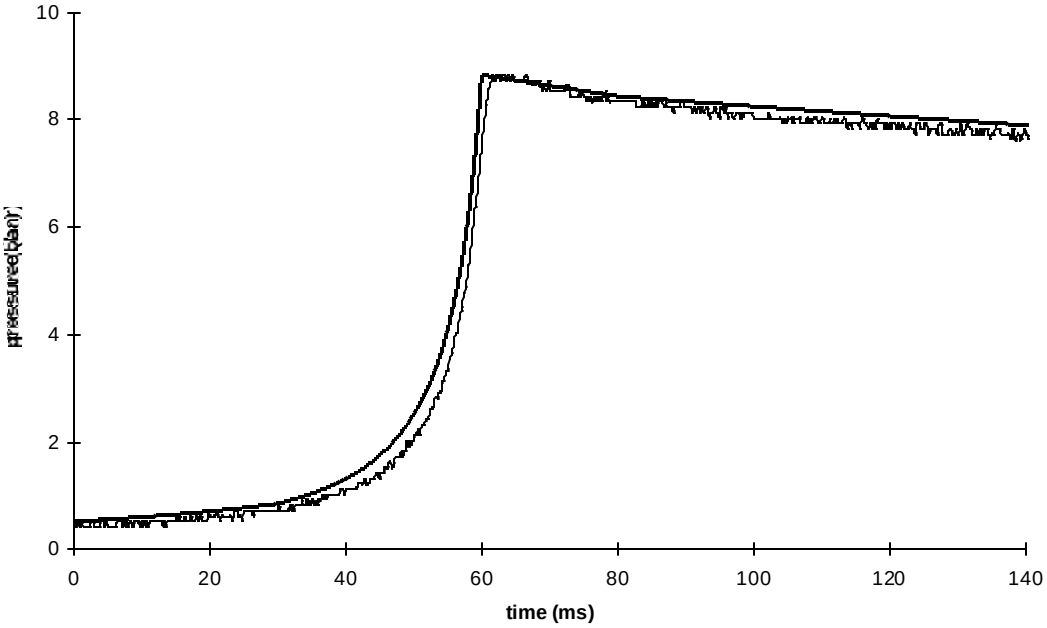

4

5

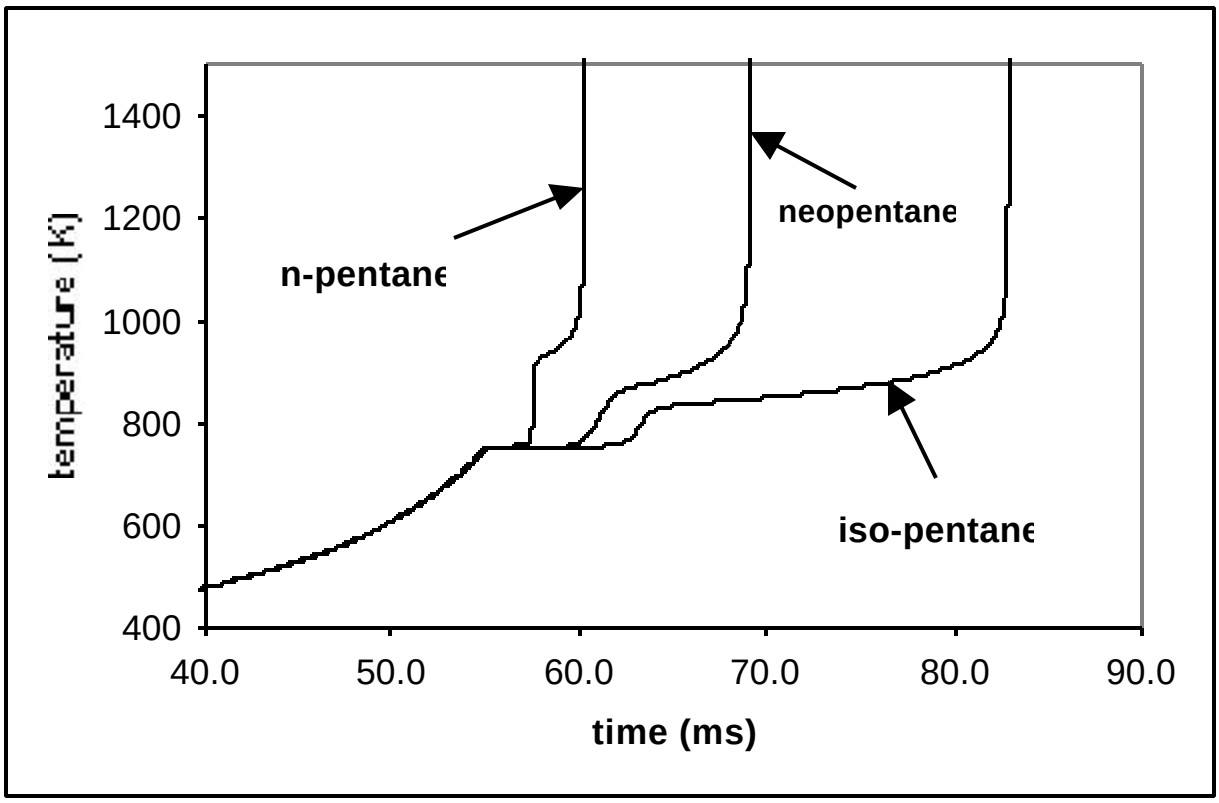
1400
1200
1000
800
600
400
temperature (K)
40.0
50.0
60.0
70.0
80.0
90.0
time (ms)
n-pentane
neopentane
iso-pentane

Table1

hydrocarbon	isopentane		neopentane		n-pentane	
RON	92.3		85.5		61.7	
p_0 / torr	300	400	300	400	300	400
T_l / K	700	690	670	665	650	650
	NTC zone		slowing down zone		NTC zone	
T_{min} / K	730	730	770	775	755	755
T_{max} / K	820	820	880	890	850	845
t_{min} / ms	75	34	21.5	5	13	6
t_{max} / ms	109	46	23.5	11	18	8
	CF zone		CF zone		CF zone	
T_{CFmin} / K	700	700	685	665	670	665
T_{CFmax} / K	755	755	880	890	840	845

Table 1 : Autoignition criteria for stoichiometric hydrocarbon / "air" mixtures